

# Integrity of Thermal Actuators using the Concept of Energy Density

C.P. Providakis<sup>1</sup>

**Abstract:** Actuators are structures that give micro-electro-mechanical systems (MEMS) the ability to interact with their environment rather than just passively sensing it. Recent studies of MEMS thermal micro-actuators have shown that simple in design and production devices can provide deflection of the order of 10  $\mu\text{m}$  at low voltages. Recently, metals and single-crystal silicon materials were included in the range of materials used for thermal actuators since they operate at lower temperatures than the commonly used (poly)silicon devices. These actuators are liable to meet the loads in service, so the corresponding integrity and stability analysis constitutes a topic of interest on which researchers have reported many significant results. Of concern are the group of homogeneous actuators, in which a temperature difference is set between the two thermal bimorph arms that are vulnerable to cracking at the micro-, meso- and macro-scale levels. The main objective of this work is to examine how, when and where failure would occur necessitates the simultaneous description of failure initiated locally and terminated globally. Up to this date, one of the most known theories used to address sub-critical and critical fracture simultaneously is the strain energy density concept. In this work potential failure sites are determined with consideration given to the influence of load, geometry and voltage potential with the use of the local and global peaks and valleys of the strain energy density distribution estimated after a finite element analysis.

**Keyword:** Micro-electromechanical systems, strain energy density, finite element, stability, failure index.

## 1 Introduction

This paper presents MEMS actuators that operate on the principle of thermal expansion with the thermal power produced by ohmic heating. These thermo-mechanical actuators operate by differential thermal expansion caused by ohmic heating in U-shaped beam of the actuator. This feature can be considered as an enrichment of the abilities of the electrostatic actuators, another major category of MEMS actuators. Electrostatic actuators can provide pressure, equally simple to design to the conventional electrostatic actuators and operate at voltage levels that are directly compatible with conventional integrated electronics.

Generally speaking, there are three categories of thermal actuators. The first category considers actuators that are activated by using an asymmetrical thermal expansion of two beams with different widths (Comtois and Bright (1997) ; Kolesar, Ko, Howard, Alen, Wilken, Boydson, Ruff and Wilks (2000); Pan and Hsu (1997)). The second category consists of actuators, which apply the bimetallic effect in order to generate a lateral deflection [Huang and Lee (1999)]. In the last category of thermal actuators is made use of asymmetric expansion of two arms obtained from four U-shaped cantilevers to provide a deflection of the silicon platform [Hoffman, Kopka and Voges (1999)].

Numerous MEMS devices have been developed that use metal single-crystal silicon and (poly)silicon as the major structural material. The presently investigated micro-electro-thermal actuator is a U-shaped MEMS device fabricated from polycrystalline silicon. It is based in the existence of a differential thermal expansion between the thin arm (hot arm) and the wide arm (cold arm) to generate deflection (Riethmuller and Bennecke(1988); Lerch, Slimane, Romanowicz and

---

<sup>1</sup> Department of Applied Sciences, Technical University of Crete, Chania, Greece.

Renaud (1996); Lott, McLain, Harb and Howell (2002); Enikov, Lazarov and Gonzales(2002), Emikov and Lazarov (2003)). A bending moment is created in the two arms and the structure deflects towards the arm with smaller expansion.

The demand for functional actuator has required a fundamental understanding of the damage and cracking behaviour of such devices. This leads to a revival of research interest in the fracture mechanics of micro-mechanical systems. Among them different criteria have been proposed to assess the field solutions as well as the experiment results. The stress intensity factor and the energy release rate concepts are used in a number of works. Recently, efforts have been made to establish the strain energy density formulation of smart devices. The strain energy density theory is capable of addressing sub-critical and critical failure simultaneously in addition to providing information on thresholds on material properties and structural design. What has been identified in many of the past works is that the peaks and valleys of strain energy density distribution can be associated with failure by yielding and failure by fracture. Their amplitudes and locations would depend on reference coordinates whether viewed locally or globally. This concept has been applied successfully to study failure instability fracture in a variety of problems [Sih and Chue (1988); Sih and Hong(1989); Chu and Ko (1989); Chao and Shie (1990)].

In this paper the strain energy concept is used to analyse the instability of a thermal actuator under different geometrical configuration of its two arms.

## 2 Statement of the problem

A typical U-shaped micro-electrothermal actuator is shown in Figure 1. This device is made by polycrystalline silicon to achieve a higher electrical resistivity. The entire actuator consists of two arms of uneven width joined at their end, with a gap between them in order to form the U shape. This physical arrangement constrains the actuator top to move laterally in an arching motion towards the cold arm side. Current flows through the thin (hot) arm and the wide (cold) arm because of a

potential difference applied across two electrical pads. The electrical current density is different in the thin and wide arm since they have different width. Thus, a lateral deflection of the tip of the actuator is generated through the bending deformation leading from the different thermal expansion of the two arms.

The properties of the material of the micro actuator are as follows:  $E = 158 \times 10^3 \text{MPa}$ ,  $\nu = 0.23$ ,  $\alpha = (\text{coefficient of thermal expansion}) = 3 \times 10^{-6} / ^\circ\text{K}$ ,  $k(\text{thermal conductivity}) = 140 \times 10^6 \text{pw}/\mu\text{m} \cdot ^\circ\text{K}$ ,  $R(\text{resistivity}) = 2.3 \times 10^{-11} \text{Tohm} \cdot \mu\text{m}$

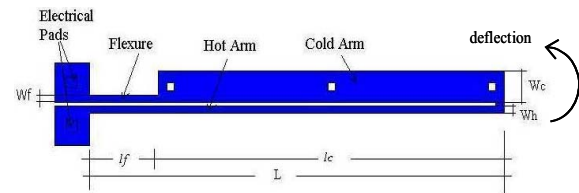


Figure 1: Geometry of the thermal microactuator

A coupled electrical-thermal mechanical transient analysis was performed using the general purposed finite element code MSC.MARC [MSC MARC (2005)]. This coupled transient analysis basically combines electrical-thermal analysis (Joule heating) with thermal-mechanical analysis. MSC.MARC 2005 uses a staggered solution procedure where the electrical problem is solved first for the nodal voltages. Next, the thermal problem is solved to obtain the nodal temperatures. Finally, the mechanical problem is solved to compute the nodal displacements.

Coupling between the electrical and thermal analysis (Joule heating) is coming from the heat generation due to electrical flow  $Q^E$ . On the other hand, coupling between thermal and mechanical problems is achieved through thermal strain loads  $F^T$  and mechanical stiffness  $K^M$ .

The equations that govern the present coupled electrical-thermal-mechanical problem can be expressed as (Sun, Gu and Carr (1996); Hsu (1983)):

$$\begin{aligned} K^E(T)V &= I \\ C^T(T)\dot{T} + K^T(T)T &= Q + Q^E \\ M\ddot{u} + D\dot{u} + K^M(T, u, t)u &= F + F^T \end{aligned} \quad (1)$$

where  $V$  is the nodal voltage vector,  $T$  is the nodal temperature vector,  $u$  is the nodal displacement vector,  $K^E(T)$  is the temperature-dependent electrical conductivity matrix,  $I$  is the nodal current vector,  $C^T(T)$  is the temperature-dependent heat capacity matrix and  $K^T(T)$  is the temperature-dependent thermal conductivity matrix. The vectors  $Q$ ,  $Q^E$ ,  $F$  and  $F^T$  are the heat flux, heat generation due to electrical flow, externally applied force and force due to thermal strain vectors, respectively.

### 3 Global and local instability

Failure by fracture in a solid could occur slowly and localized or quickly and wide spread. According to the strain energy density theory, such behavior can be evaluated from the stationary values of the energy density  $dW/dV$  and the index  $\lambda$ , which is the distance between points of the local and global minima of  $dW/dV$ . This length parameter  $\lambda$  was introduced and associated with changes in the system stability when material and geometric parameters are altered for different loading [Sih and Chue (1988)]. For a system with small index  $\lambda$  is more contained and therefore is more stable as compared with a system having a larger  $\lambda$ .

For a problem with known stresses the stationary values of the strain energy density function can be evaluated from the expression [Sih (1982)]:

$$\frac{dW}{dV} = \frac{1}{2E} [(1+\nu)\sigma_{ij}\sigma_{ij} - \nu\sigma_{kk}^2] \quad (2)$$

The strain energy density criterion of failure by fracture states that the location of fracture coincides with the local maximum of the relative minimum of strain energy density  $[(dW/dV)_{\min}^{\max}]_L$  at point  $L$ . It is assumed that fracture initiation occurs when  $[(dW/dV)_{\min}^{\max}]_L$  reaches a critical value  $(dW/dV)_{cr}$ . Once failure by fracture has initiated it is also assumed that fracture tends toward the location of maximum of global minimum  $[(dW/dV)_{\min}^{\max}]_G$  at point  $G$ .

To facilitate the determination of points  $L$  and  $G$ , in the present paper MSC.MARC program is used to compute and plot the strain energy

density  $dW/dV$  contours. This provides a visual identification of  $L$  and  $G$  locations with a quick graphical topographic mapping procedure. Let  $L$  coincides with the point of failure initiation. Assume that here it could be the location where  $[(dW/dV)_{\min}^{\max}]$  appears to reach the maximum computed value. The predicted length parameter  $\lambda = (LG)$  corresponds to the loci of the points that start from point  $L$  and connects all those having the maximum gradient of  $(dW/dV)$ . The end point is  $G$ , where the global minimum value of  $(dW/dV)$  prevails. On the MSC.MARC resulted topographic map, the parameter  $\lambda$  is indicated by joining the above mentioned points by a line, resulting in a curve, which starts from the peak  $L$  and ends in vicinity of the point  $G$ .

The length  $l = (LG)$  of the arc between the local  $L$  and global  $G$  minima of the strain energy density function  $dW/dV$  can, then, be considered as an index that determines the length of the unstable fracture path and serves as a measure of the stability of the fracture. As Sih [11] has proposed, the interaction between the values of  $\lambda$  and  $[(dW/dV)_{\min}^{\max}]_L$  controls the fracture instability of the structure in a manner described as below:

Fracture is localized if the index  $\lambda$  decreases with increasing  $[(dW/dV)_{\min}^{\max}]_L$ . The initial fracture will spread and the structure could result in global failure if the index  $\lambda$  increases with increasing  $[(dW/dV)_{\min}^{\max}]_L$ .

#### 3.1 Specimen geometry and strain analysis

To perform a stress analysis, the microelectrothermal actuator of Figure 1 is discretized by using four noded isoparametric elements with four Gaussian integration points. Since there is no symmetry the entire actuator should be considered. The mesh consists of 3176 elements with 7208 nodes. The transient electro-thermo-mechanical and strain distribution is computed by using the general purpose finite element code MCS. MARC [MSC MARC (2005)].

The values of strain energy density  $[(dW/dV)_{\min}^{\max}]_L$  and  $[(dW/dV)_{\min}^{\max}]_G$  were obtained together with the corresponding locations of the points  $L$  and  $G$  from the contours of strain energy per unit volume. Numerical results

are obtained for the index of instability  $\ell$  for a variety of the width values  $W_f$  of the flexure portion of the cold arm (see Figure 1). This is achieved, while holding the other geometric parameters such as  $W_c, L, l_f, l_c$  fixed, respectively, at 2 and 16 microns wide and 240, 40 and 200 microns long, respectively. The gap between the hot and cold arm is also fixed at 2 microns wide. The thickness of the actuator is 2 microns. The initial temperature of the actuator is fixed at 300 °K. The electrical pads at the top of the two ends of the arms were loaded with a potential difference linearly time-varied from 0 to 5 volts. The electrical pads are assumed to be fixed in all three displacement directions.

#### 4 Numerical results

Seven sets of calculations were made for seven different widths  $W_f$  of the flexure portion of the cold arm: 1.25, 1.5, 1.75, 2, 2.5, 3.5, 4.5 microns. For each set we obtain only the local and global maximum of the relative minima of  $dW/dV$ . At a given electrical potential difference increment the actuator possesses a pair of the local and global  $(dW/dV)_{\min}^{\max}$  stationary values. The distances between these stationary values here denoted by  $\ell_j$ . A typical contour plot of the energy density function is shown in Figure 2.

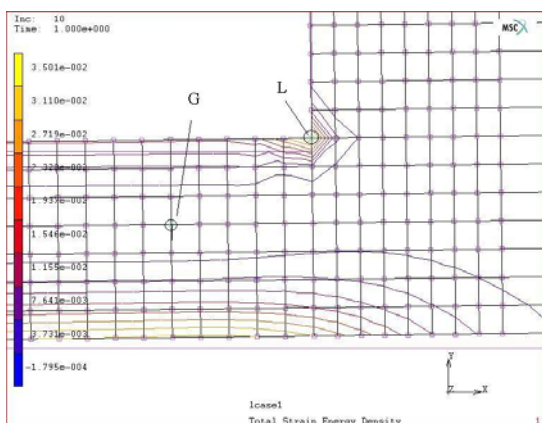


Figure 2: Location of points  $L$  and  $G$  in the flexure portion of cold arm.

The contours given in Figure 2 are depicted for

increment 10 and width  $W_f = 3.5$  microns and show that  $dW/dV$  near the right angle of the flexure portion of the actuator reached . 0.0350127 at point  $L$  while lowest energy density occurs at a point  $G$ . The distance  $\ell$  between those two points  $L$  and  $G$  serves as an approximate ranking of failure instability. Numerical results of the variation of  $[(dW/dV)_{\min}^{\max}]_L$  and  $\ell$  as a function of the width  $W_f$  is depicted in Figures 3-6 for the increments 4, 6, 8 and 10, which are selected because could indicate in a more elaborated fashion the non-monotonic variation of index  $\lambda$  with width  $W_f$ .

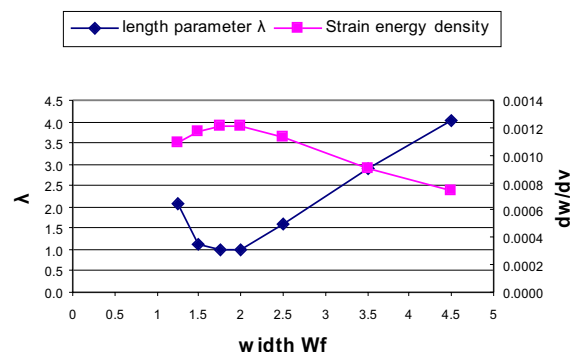


Figure 3: Values of  $dW/dV$  and index  $\lambda$  as a function of width  $W_f$  for increment 4.

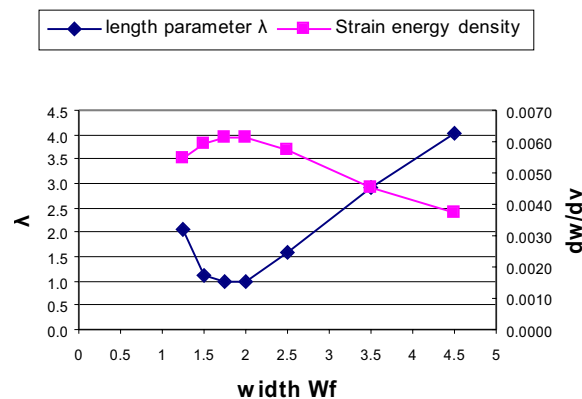


Figure 4: Values of  $dW/dV$  and index  $\lambda$  as a function of width  $W_f$  for increment 6.

The failure instability behavior is different when  $W_f$  takes on different values. There exist a minimum of the distance  $\ell$  between  $L$  and  $G$ . This is

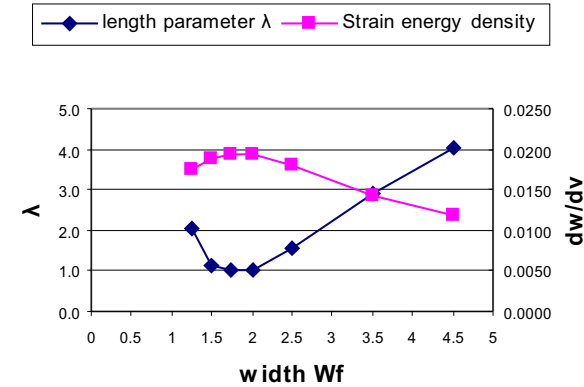


Figure 5: Values of  $dW/dV$  and index  $\lambda$  as a function of width  $W_f$  for increment 8.

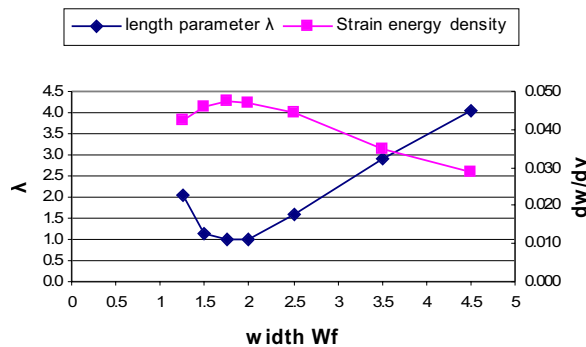


Figure 6: Values of  $dW/dV$  and index  $\lambda$  as a function of width  $W_f$  for increment 10.

shown in all the Figures 3-6. A minimum  $\lambda$  occurs at width  $W_f \cong 1.75$  microns beyond which distance  $\lambda$  would increase. At the same time a maximum of the local strain energy at point  $L$  corresponds for the same the value of  $W_f \cong 1.75$  microns. After the value of  $W_f \cong 1.75$  the strain energy at point  $L$  becomes less intensified as the flexure portion of the cold arm of the actuator is increased, a result that is expected.

The non-monotonic variation of  $\lambda$  with  $W_f$  shows how the mere change of a single geometric parameter could alter the failure behavior from stable to. The index of fracture instability, however, behaves in the opposite direction. It increases with increasing  $W_f$  after the value of  $W_f \cong 1.75$  microns.

## 5 Conclusions

Application of the strain energy density criterion is performed to investigate the failure instability of micro-electro-thermal actuators containing localized changes in the geometrical characteristics of its arms. The length parameter  $\lambda$  between the maximum of the local minima of  $dW/dV$ ,  $L$ , and the global minimum of  $dW/dV$ ,  $G$  was measured to characterize the fracture instability of the actuator. It should be determined in the actuator design against fracture. For optimal design,  $\lambda$  should be kept as small as possible. Variation of  $\lambda$  and  $[(dW/dV)_{\min}^{\max}]_L$  with reference to the flexure width of the cold arm of the actuator could appose one another. This is desirable because high  $[(dW/dV)_{\min}^{\max}]_L$  increases the possibility of fracture initiation while small  $\lambda$  corresponds to less wide spread fracture.

## References

- Chao, C.K. ; Shie, J.J.** (1990): Stability of failure initiation by fracture for a bimaterial body with an edge crack, *Theor. Appl. Fract. Mech.*, vol. 14, pp. 123-133.
- Chu, R.C. ; Ko, T.C.**, (1989): Isoparametric shear spring element applied to crack patching and instability, *Theor. Appl. Fract. Mech.*, vol. 11, pp.93-102.
- Comtois, J.H. ; Bright, V.M.** (1997): Applications for surface-micromachined polysilicon thermal actuators and arrays, *Sensors & Actuators A*, vol. 58, pp.19-25.
- Enikov, E.T.; Lazarov, K.V.; Gonzales, G.R.**, (2002): Microelectrical mechanical systems actuator array for tactile communication, In *ICCHP 2002 Lecture Notes in Computer Science*, vol. 2398, pp. 251-558.
- Enikov, E.T. ; Lazarov, K.**, (2003): PCB-integrated metallic thermal micro-actuators, *Sens. Actuators*, vol. 105, pp. 76-82.
- Hoffman, M; Kopka, P. ; Voges, E.**(1999): Bistable micromechanical fiber-optic switches on silicon with thermal actuators, *Sens. Actuators*, vol. 78.
- Hsu, M.B.**, (1983): Modeling of coupled thermo-

electrical problems by the finite element method, In *Proceedings of 3<sup>rd</sup> International Conf. Numer. Meths in Engng.*, Paris.

**Huang, Q.A. ; Lee, N.K.S.** (1999): Analysis and design of polysilicon thermal flexure actuator, *J. Micromech. Microeng.*, **9**, pp. 64-70.

**Kolesar, E.S. ; Ko, S.Y. ; Howard, J.T. ; Allen, P.B. ; Wilken, J.M. ; Boydston, N.C. ; Ruff, M.D. ; Wilks R.J.** (2000): In-plane tip deflection and force achieved with asymmetrical polysilicon electrothermal microactuators, *Thin Solid Films*, vol. 377-378, pp. 719-726, 2000.

**Lerch, P. ; Slimane, C.K. ; Romanowicz, B. ; Renaud, P.** (1996) : Modelization and characterization of asymmetrical thermal micro-actuators, *Microengngn.*, vol. 6, pp. 134-137.

**Lott, C.D.; McLain, T.W.; Harb, J.N.; Howell, L.L.**, (2002): Modeling the thermal behavior of a surface-micromachined linear-displacement thermomechanical microactuator, *Sens. Actuators*, vol. 101, pp. 239-250.

**MSC.MARC 2005**, Users Guide, MSC.Software, CA, USA.

**Pan, C.S. ; Hsu, W.** (1997): An electro-thermally and laterally driven polysilicon microactuator, *J. Micromech. Microeng.*, vol. 7, pp. 7-13.

**Riethmuller, W.; Benecke, W.**, (1988): Thermally excited silicon microactuators, *IEEE Trans. Electron devices*, vol. 35(6), pp. 64-70.

**Sih, G. ; Chue, C.H.**, (1988): Stability and integrity of mechanical joints in flight vehicles: Local and Global energy density, *Theor. Appl. Fract. Mech.*, vol. 10, pp. 135-149.

**Sih, G. ; Hong, T.B.** (1989): Integrity of edge-debonded patch in cracked panel, *Theor. Appl. Fract. Mech.*, vol. 12, pp. 121-139.

**Sih, G.C. ; Chue, C.H.** (1988): Stability and integrity of mechanical joints in flight vehicles: Local and global energy density, *Theor. Appl. Fract. Mech.*, vol. 10, pp. 135-149.

**Sih, G.C.**, (1990): Introductory chapters In: G.C. Sih (Ed.) *Mechanics of Fracture*, I-VII, Martinus Nijhoff, , The Netherlands.

**Sun, X.Q.; Gu, X.; Carr, X.**, (1996): Lateral in-plane displacement micro-actuator with com-

bined thermal and electrostatic drive, In *Proceedings of the Solid State Sensor and Actuator Workshop*, Hilton Head, S. Carolina.